

Comparing bias correction methods in downscaling meteorological variables for hydrologic impact study in an arid area in China

G.H. Fang^{1,2,3}, J. Yang^{1*,4}, Y.N. Chen¹, C. Zammit⁴

¹ State Key Laboratory of Desert and Oasis Ecology, Xinjiang Institute of Ecology and Geography, Chinese Academy of Sciences, Xinjiang, China

² University of Chinese Academy of Sciences, Beijing, China

³ Department of Geography, Ghent University, Ghent, Belgium

⁴ National Institute of Water and Atmospheric Research, Christchurch, New Zealand

Corresponding author:

Jing Yang*

State Key Laboratory of Desert and Oasis Ecology, Xinjiang Institute of Ecology and Geography, Chinese Academy of Sciences, Xinjiang, 830011, China

818 South Beijing Road, Urumqi, Xinjiang, 830011, China

Tel: +86-991-7823171

Email: yangjing@ms.xjb.ac.cn

1 **Comparing bias correction methods in downscaling meteorological variables for**
2 **hydrologic impact study in an arid area in China**

3 **Abstract:**

4 Water resources are essential to the ecosystem and social economy in the desert
5 and oasis of the arid Tarim River Basin, Northwest China, and expected to be
6 vulnerable to climate change. Regional Climate Models (RCM) have been proved to
7 provide more reliable results for regional impact study of climate change (e.g., on
8 water resources) than GCM models. However, it is still necessary to apply bias
9 correction before they are used for water resources research due to often considerable
10 biases. In this paper, after a sensitivity analysis on input meteorological variables based
11 on Sobol' method, we compared five precipitation correction methods and three
12 temperature correction methods to the output of a RCM model with its application to
13 the Kaidu River Basin, one of the headwaters of the Tarim River Basin. Precipitation
14 correction methods include Linear Scaling (LS), LOCal Intensity scaling (LOCI),
15 Power Transformation (PT), Distribution Mapping (DM) and Quantile Mapping (QM);
16 and temperature correction methods include LS, VARIance scaling (VARI) and DM.
17 These corrected precipitation and temperature were compared to the observed
18 meteorological data, and then their impacts on streamflow were also compared by
19 driving a distributed hydrologic model. The results show: 1) Precipitation, temperature,
20 solar radiation are sensitivity to streamflow while relative humidity and wind speed are
21 not; 2) Raw RCM simulations are heavily biased from observed meteorological data,

22 which results in biases in the simulated streamflows, and all bias correction methods
23 effectively improved these simulations; 3) For precipitation, PT and QM methods
24 performed equally best in correcting the frequency-based indices (e.g., standard
25 deviation, percentile values) while LOCI method performed best in terms of the time
26 series based indices (e.g., Nash-Sutcliffe coefficient, R^2); 4) For temperature, all bias
27 correction methods performed equally well in correcting raw temperature. 5) For
28 simulated streamflow, precipitation correction methods have more significant influence
29 than temperature correction methods and the performances of streamflow simulations
30 are consistent with these of corrected precipitation, i.e., PT and QM methods
31 performed equally best in correcting flow duration curve and peak flow while LOCI
32 method performed best in terms of the time series based indices. The case study is for
33 an arid area in China based on a specific RCM and hydrologic model, but the
34 methodology and some results can be applied to other area and other models.

35

36

37 **1. Introduction**

38 In recent decades, the ecological situation of the Tarim River Basin in China has
39 seriously degraded especially in the lower reaches of the Tarim River due to water
40 scarcity. In the meantime, climate change is significant in this region with a consistent
41 increase in temperature at a rate of 0.33 ~ 0.39 °C/decade and a slight increase in
42 precipitation (Li et al., 2012) over the past 5 decades. Under the context of regional
43 climate change, water resources in this region are expected to be more unstable and
44 ecosystems are likely to suffer from severe water stress because the hydrologic system
45 is particularly vulnerable to climate change in the arid region (Arnell et al., 1992; Shen
46 and Chen, 2010; Sun et al., 2013; Wang et al., 2013). The impact of climate change on
47 hydrologic system has already been observed and it is expected that the hydrological
48 system will continue to change in the future (Liu et al., 2011; Liu et al., 2010; Chen et
49 al., 2010). Therefore, projecting reliable climate change and its impact on hydrology
50 are important to study the ecology in the Tarim River Basin.

51 Only recently efforts have been made to evaluate and project the impact of
52 climate change on hydrology in the Tarim River Basin. These studies include research
53 on the relationships of climate variables and streamflow based on the historical
54 measurements (e.g. Chen et al., 2013c; Xu et al., 2013), and use of the output of
55 General Circulation Models (GCMs) to drive a hydrologic model to study the future
56 climate change on water resources (Liu et al., 2010; Liu et al., 2011). Study on
57 historical relationships has limited applications on future water resource management,
58 especially under the global climate change background. And though GCMs have been

59 widely used to study impacts of future climate change on hydrological systems and
60 water resources, they are impeded by their inability to provide reliable information at
61 the hydrological scales (Maraun et al., 2010; Giorgi, 1990). In particular, in
62 mountainous regions, fine scale information such as the altitude-dependent
63 precipitation and temperature information, which is critical for hydrologic modeling, is
64 not represented in GCMs (Seager and Vecchi, 2010). Although there are options to
65 downscale GCM outputs to the regional scale, recent studies tend to use the
66 higher-resolution Regional Climate Models (RCMs) to preserve the physical coherence
67 between atmospheric and land surface variables (Bergstrom et al., 2001; Anderson et
68 al., 2011). As such, when evaluating the impact of climate change on water resources
69 in a watershed scale, the use of RCMs instead of GCMs is preferable since RCMs have
70 been proved to provide more reliable results for impact study of climate change on
71 regional water resources than GCM models (Buytaert et al., 2010; Elguindi et al.,
72 2011). However, the raw RCM simulations may be still biased especially in the
73 mountainous regions (Murphy, 1999; Fowler et al., 2007), which makes the use of
74 RCM outputs as the direct input for hydrological model challenging, thus it is of
75 significance to properly correct the RCM simulated meteorological variables before
76 they are used to drive the hydrological model especially in the arid regions where the
77 hydrology is sensitive to climate change.

78 Several bias correction methods have been developed to downscale climate
79 variables from the RCMs, ranging from the simple scaling approach to sophisticated
80 distribution mapping (Teutschbein and Seibert, 2012). And their applicability in the

81 arid Tarim River Basin has not been investigated, thereby, evaluating and finding the
82 appropriate bias correction method is necessary to evaluate the impact of climate
83 change to water resources.

84 This study evaluates performances of five precipitation bias correction methods
85 and three temperature bias correction methods in correcting RCM simulations and
86 applied to the Kaidu River Basin, one of the most important headwaters of the Tarim
87 River. These bias correction methods include most frequently used bias correction
88 methods. We compare their performances in terms of precipitation and temperature and
89 evaluate their impact on streamflow through hydrological modeling.

90 The remaining is constructed as follows: Section 2 introduces the study area and
91 data; Section 3 describes the bias correction methods for precipitation and temperature
92 along with the hydrological model, sensitivity analysis method and result analysis
93 strategy; and then Section 4 gives results and discussion, followed by conclusions in
94 Section 5.

95

96 **2 Study area and data**

97 2.1 Study area and observed data

98 The Kaidu River Basin, with a drainage area of 18,634 km² above the Dashankou
99 hydrological station, is located on the south slope of the Tianshan Mountains in
100 Northwest China (Fig. 1). Its altitude ranges from 1,340 m to 4,796 m above sea level
101 (asl) with an average elevation of 2,995 m, and climate is featured by temperate

102 continental climate with alpine climate characteristic. As one of the headwaters of the
103 Tarim River, it provides water resources for agricultural activity and ecological
104 environment of the oasis in the lower reaches. This oasis, with a population of over
105 1.15 million, is stressed by lack of water and water resources are the main factor
106 constricting the development (Chen et al., 2013b). Therefore, projecting the impact of
107 future climate change on water resources is urgent to the sustainable development of
108 this region.

109 Daily observed meteorological data, including precipitation, maximum/minimum
110 temperature, wind speed and relative humidity of two meteorological stations
111 (Bayanbulak and Baluntai, stars in Figure 1), are from the China Meteorological Data
112 Sharing Service System (<http://cdc.cma.gov.cn/>). The mean annual maximum and
113 minimum temperature at the Bayanbulak meteorological station are 3.1 °C and
114 -10.6 °C and mean annual precipitation is 267 mm, and generally precipitation falls as
115 rain from May to September and as snow from October to April of the next year.

116 The observed streamflow data at the Dashankou hydrologic station (the triangle in
117 Figure 1) are from Xinjiang Tarim River Basin Management Bureau. The average daily
118 flow is around 110 m³ s⁻¹ (equivalent to 185 mm runoff/year), ranging from 15 m³ s⁻¹ to
119 973 m³ s⁻¹.

120 2.2 Simulated meteorological variables from the regional climate model

121 GCM or RCM outputs are generally biased (Ahmed et al., 2013;Teutschbein and
122 Seibert, 2012;Mehrotra and Sharma, 2012), which demonstrates the need for bias

123 correction before their use in regional impact studies. The RCM outputs used in this
124 study are based on the work done by Gao et al (2013). In Gao et al. (2013), the RCM
125 model (RegCM, Giorgi and Mearns, 1999) was driven by a global climate model
126 BCC_CSM1.1 (Beijing Climate Center Climate System Model; Wu et al., 2013; Xin et
127 al., 2013) at a horizontal resolution of 50 km over China.

128 The RCM outputs were validated with the observational dataset (CN05.1) over
129 China for the period from 1961 to 2005. The RCM outputs show reasonable simulation
130 of temperature and precipitation over China especially when compared with its driving
131 GCM BCC_CSM1.1 (more details refer to Gao et al., 2013). In this paper,
132 meteorological outputs of the RCM model used include maximum/minimum
133 temperature, precipitation, wind speed, solar radiation and humidity.

134 **3 Methodology**

135 3.1 Hydrologic model and sensitivity of input meteorological variables

136 SWAT (Soil and Water Assessment Tool; Arnold et al., 1998) is a distributed and
137 time continuous watershed hydrologic model. The climatic input (driving force)
138 consists of daily precipitation, maximum/minimum temperature, solar radiation, wind
139 speed and relative humidity, and SWAT uses elevation bands to account for orographic
140 effects on precipitation and temperature. The processes SWAT simulates include snow
141 accumulation, snowmelt, evapotranspiration, surface runoff, lateral flow, and baseflow,
142 sediment erosion, point and non-point pollution, river routing and in-stream water
143 quality processes on a daily basis. More details refer to SWAT manuals

144 (www.brc.tamus.edu/). It has been being widely used for comprehensive modeling of
145 the impact of management practices and climate change on the hydrologic cycle and
146 water resources at a watershed scale (e.g. Arnold et al., 2000; Arnold and Fohrer, 2005;
147 Setegn et al., 2011).

148 In this study, SWAT model was firstly set up with available DEM, landuse, soil,
149 and observed climate data, and then model parameters were calibrated with the
150 observed streamflow data at the Dashankou station. The simulation results show: 1)
151 model application shows excellent performances for both calibration period (1986 ~
152 1989) and validation period (1990 ~ 2001) with “NS”s (Nash-Sutcliffe coefficients,
153 Nash and Sutcliffe, 1970; see the definition in Eq. 16) and “R²”s over 0.80, which is
154 highly acceptable; 2) model parameters are reasonable and spatial patterns of
155 precipitation and temperature are in agree with other studies in the region (see more
156 details in Fang et al., under submission). Figure 2 shows a comparison of mean
157 hydrographs of the observed (“obs”) and simulated flows (“default”). This calibrated
158 model hence provides a basis for evaluation of the impact of different correction
159 methods on streamflow.

160 To study the relative importance of the five meteorological variables, the Sobol’
161 sensitivity analysis method (Sobol’, 2001) was applied. The Sobol’ method is based on
162 the decomposition of the variance V of objective function:

$$163 \quad V = \sum_i V_i + \sum_i \sum_{j>i} V_{ij} + \cdots + V_{1,2,\dots,n} \quad (1)$$

164 where

$$165 \quad V_i = V(\mu(Y|X_i))$$

166 $V_{ij} = V\left(\mu(Y|X_i, X_j)\right) - V_i - V_j$

167 and so on. Herein, $V(.)$ denotes the variance operator, V is the total variance, and V_i
 168 and V_{ij} are main variance of X_i (the i^{th} factor of X) and partial variance of X_i and X_j .
 169 Here factors X are the changes applied to these five meteorological variables,
 170 respectively (see Table 1 for a list of these factors). In practice, normalized indices are
 171 often used as sensitivity measures:

172 $S_i = \frac{V_i}{V}, 1 \leq i \leq n$ (2)

173 $S_{ij} = \frac{V_{ij}}{V}, 1 \leq i < j \leq n$ (3)

174 $S_{Ti} = S_i + \sum_j S_{ij} + \sum_j \sum_k S_{ijk} + \dots + S_{1,2,\dots,n}, 1 \leq i \leq n$ (4)

175 Where S_i , S_{ij} and S_{Ti} are the main effect of X_i , first order interaction between X_i and X_j ,
 176 and total effect of X_i . S_{Ti} ranges from 0 to 1 and denotes the importance of the factor to
 177 model output. The larger S_{Ti} , the more important this factor is. The difference between
 178 S_{Ti} and S_i denotes the significance of the interaction of this factor with other factors. As
 179 a result, the larger this difference, the more significant the interaction is.

180 3.2 Bias correction methods

181 In this study, five bias correction methods were used for precipitation, and three
 182 for temperature. These methods are listed in Table 2. All these bias correction methods
 183 were conducted on a daily basis from 1975 to 2005.

184 3.2.1 Linear Scaling (LS) of precipitation and temperature

185 LS method aims to perfectly match the monthly mean of corrected values with
 186 that of observed ones (Lenderink et al., 2007). It operates with monthly correction

187 values based on the differences between observed and raw data (raw RCM simulated
 188 data in this case). Precipitation is typically corrected with a multiplier and temperature
 189 with an additive term on a monthly basis:

$$190 \quad P_{cor,m,d} = P_{raw,m,d} \times \frac{\mu(P_{obs,m})}{\mu(P_{raw,m})} \quad (5)$$

$$191 \quad T_{cor,m,d} = T_{raw,m,d} + \mu(T_{obs,m}) - \mu(T_{raw,m}) \quad (6)$$

192 where $P_{cor,m,d}$ and $T_{cor,m,d}$ are corrected precipitation and temperature on the d^{th} day of
 193 m^{th} month and $P_{raw,m,d}$ and $T_{raw,m,d}$ are the raw precipitation and temperature on the d^{th}
 194 day of m^{th} month. $\mu(\cdot)$ represents the expectation operator (e.g., $\mu(T_{obs,m})$
 195 represents the mean value of observed precipitation at given month m).

196

197 3.2.2 LOCal Intensity scaling (LOCI) of precipitation

198 LOCI method (Schmidli et al., 2006) corrects the wet-day frequencies and
 199 intensities and can effectively improve the raw data which have too many drizzle days
 200 (defined as days with little precipitation). It normally involves two steps: firstly, a
 201 wet-day threshold for the m^{th} month $P_{thres,m}$ is determined from the raw precipitation
 202 series to ensure that the threshold exceedance matches the wet-day frequency of the
 203 observation; secondly, a scaling factor $s_m = \frac{\mu(P_{obs,m,d}|P_{obs,m,d}>0)}{\mu(P_{raw,m,d}|P_{raw,m,d}>P_{thres,m})}$ is calculated
 204 and used to ensure that the mean of the corrected precipitation is equal to that of the
 205 observed precipitation:

$$206 \quad P_{cor,m,d} = \begin{cases} 0, & \text{if } P_{raw,m,d} < P_{thres,m} \\ P_{raw,m,d} \times S_m, & \text{otherwise} \end{cases} \quad (7)$$

207

208 3.2.3 Power Transformation (PT) of precipitation

209 While the LS and LOCI account for the bias in the mean precipitation, it does not
210 correct biases in the variance. PT method uses an exponential form to further adjust the
211 standard deviation of precipitation series. Since PT has the limitation in correcting the
212 wet day probability (Teutschbein and Seibert, 2012), which was also confirmed in our
213 study (not shown), LOCI method is applied to correct precipitation prior to the
214 correction by PT method.

215 Therefore, to implement this PT method, firstly, we estimate b_m that minimizes:

$$216 f(b_m) = \frac{\sigma(P_{obs,m})}{\mu(P_{obs,m})} - \frac{\sigma(P_{LOCI,m}^{b_m})}{\mu(P_{LOCI,m}^{b_m})} \quad (8)$$

217 where b_m is the exponent for the m^{th} month, $\sigma(\cdot)$ represents the standard deviation
218 operator, and $P_{LOCI,m}$ is the LOCI-corrected precipitation in the m^{th} month. If b_m is
219 larger than one, it indicates that the LOCI-corrected precipitation underestimates its
220 coefficient of variance in month m .

221 After finding the optimal b_m , the parameter $s_m = \frac{\mu(P_{obs,m})}{\mu(P_{LOCI,m}^{b_m})}$ is then determined

222 such that the mean of the corrected values corresponds to the observed mean. The
223 corrected precipitation series are obtained based on the LOCI corrected precipitation

224 $P_{cor,m,d}$:

$$225 P_{cor,m,d} = s_m \times P_{LOCI,m,d}^{b_m} \quad (9)$$

226

227 3.2.4 Variance scaling (VARI) of temperature

228 The PT method is an effective method to correct both the mean and the variance
229 of precipitation, but it cannot be used to correct temperature time series, as temperature

230 is known to be approximately normally distributed (Terink et al., 2010). VARI method
 231 was developed to correct both the mean and variance of normally distributed variable
 232 such as temperature (Teutschbein and Seibert, 2012; Terink et al., 2010). Temperature
 233 is normally corrected using VARI method with Eq. (10).

$$234 \quad T_{cor,m,d} = [T_{raw,m,d} - \mu(T_{raw,m})] \times \frac{\sigma(T_{obs,m})}{\sigma(T_{raw,m})} + \mu(T_{obs,m}) \quad (10)$$

235

236 3.2.5 Distribution mapping (DM) of precipitation and temperature

237 DM method is to match the distribution function of raw data to that of observation.
 238 It is used to adjust mean, standard deviation and quantiles. Furthermore, it preserves
 239 the extremes (Thiemeßl et al., 2012). However, it also has its limitation due to the
 240 assumption that both the observed and raw climate variables follow the same proposed
 241 distribution, which may introduce potential new biases.

242 For precipitation, the Gamma distribution (Thom, 1958) with shape parameter α
 243 and scale parameter β is often used for precipitation distribution and has been proven
 244 to be effective (e.g., Block et al., 2009; Piani et al., 2010):

$$245 \quad f_r(x|\alpha, \beta) = x^{\alpha-1} \times \frac{1}{\beta^\alpha \times \Gamma(\alpha)} \times e^{-\frac{x}{\beta}}; x \geq 0, \alpha, \beta > 0 \quad (11)$$

246 where $\Gamma(\cdot)$ is the Gamma function. Since the raw RCM-simulated precipitation
 247 contains a large number of drizzle days, which may substantially distort the raw
 248 precipitation distribution, the correction is done on LOCI corrected precipitation

249 $P_{LOCI,m,d}$:

$$250 \quad P_{cor,m,d} = F_r^{-1}(F_r(P_{LOCI,m,d}|\alpha_{LOCI,m}, \beta_{LOCI,m})|\alpha_{obs,m}, \beta_{obs,m}) \quad (12)$$

251 Where $F_r(\cdot)$ and $F_r^{-1}(\cdot)$ are Gamma CDF (cumulative distribution function) and its

252 inverse. $\alpha_{LOCI,m}$ and $\beta_{LOCI,m}$ are the fitted Gamma parameter for the LOCI
 253 corrected precipitation in a given month m , and $\alpha_{obs,m}$ and $\beta_{obs,m}$ are these for
 254 observation.

255 For temperature, the Gaussian distribution (or normal distribution) with mean μ
 256 and standard deviation σ is usually assumed to fit temperature best (Teutschbein and
 257 Seibert, 2012):

$$258 \quad f_N(x|\mu, \sigma) = \frac{1}{\sigma\sqrt{2\pi}} \times e^{-\frac{(x-\mu)^2}{2\sigma^2}}; x \in \mathbf{R} \quad (13)$$

259 And then similarly the corrected temperature can be expressed as:

$$260 \quad T_{cor,m,d} = F_N^{-1}(F_N(T_{raw,m,d}|\mu_{raw,m}, \sigma_{raw,m})|\mu_{obs,m}, \sigma_{obs,m}) \quad (14)$$

261 where $F_N(\cdot)$ and $F_N^{-1}(\cdot)$ are Gaussian CDF and its inverse, $\mu_{raw,m}$ and $\mu_{obs,m}$ are
 262 the fitted and observed means for the raw and observed precipitation series at a given
 263 month m , and $\sigma_{raw,m}$ and $\sigma_{obs,m}$ are the corresponding standard deviations,
 264 respectively.

265

266 3.2.6 Quantile Mapping (QM) of precipitation

267 QM method is a non-parametric bias correction method and is generally
 268 applicable for all possible distributions of precipitation without any assumption on
 269 precipitation distribution. This approach originates from the empirical transformation
 270 (Thiemeß et al., 2012) and was successfully implemented in the bias correction of
 271 RCM simulated precipitation (Sun et al., 2011; Thiemeß et al., 2012; Chen et al., 2013a;
 272 Wilcke et al., 2013). It can effectively correct bias in the mean, standard deviation and
 273 wet day frequency as well as quantiles.

274 For precipitation, the adjustment of precipitation using QM can be expressed in
275 terms of the empirical CDF (*ecdf*) and its inverse (*ecdf⁻¹*):

$$276 P_{cor,m,d} = ecdf_{obs,m}^{-1}(ecdf_{raw,m}(P_{raw,m,d})) \quad (15)$$

277

278 3.3 Performance evaluation

279 The performance evaluation of these correction methods is based on their abilities
280 to reproduce precipitation, temperature, and streamflow simulated with a hydrological
281 model (SWAT) driven by bias corrected RCM simulations, specifically. When
282 evaluating ability to reproduce streamflow, streamflow is firstly simulated by running
283 the hydrological model driven by 15 different combinations of corrected precipitation,
284 max/min temperature with different correction methods (these hydrologic simulations
285 are then referred to as simulations 1 to 15, which are listed in Table 3) together with
286 hydrologic simulations driven by observed meteorological data (“default”) and raw
287 RCM simulation (“raw”). These 15 simulations were then compared with observed
288 streamflows and “default” and “raw”.

289 The performance evaluation of precipitation, temperature and streamflow with
290 different correction methods are:

291 1) For corrected precipitation, frequency-based indices and time series
292 performances are compared with observed precipitation data. The frequency-based
293 indices include mean, median, standard deviation, 90th percentile, probability of wet
294 days, and intensity of wet day while time series based metrics include NS, Percent bias

295 (P_{BIAS}), R^2 and Mean Absolute Error (MAE):

$$296 \quad NS = 1 - \frac{\sum_{i=1}^n (Y_i^{obs} - Y_i^{sim})^2}{\sum_{i=1}^n (Y_i^{obs} - Y^{mean})^2} \quad (16)$$

$$297 \quad P_{BIAS} = \frac{\sum_{i=1}^n (Y_i^{obs} - Y_i^{sim})}{\sum_{i=1}^n (Y_i^{obs})} \quad (17)$$

$$298 \quad MAE = \frac{\sum_{i=1}^n |Y_i^{obs} - Y_i^{sim}|}{n} \quad (18)$$

299 Where Y_i^{obs} and Y_i^{sim} are the i^{th} observed and simulated variables, Y^{mean} is the mean of
300 observed variables, and n is the total number of observations.

301 NS indicates how well the simulation matches the observation and it ranges
302 between $-\infty$ and 1.0, with $NS = 1$ meaning a perfect fit. The higher this value, the more
303 reliable the model is. P_{BIAS} measures the average tendency of the simulated data to
304 their observed counterparts. Positive values indicate an overestimation of observation,
305 while negative values indicate an underestimation. The optimal value of P_{BIAS} is 0.0,
306 with low-magnitude values indicating accurate model simulations.

307 2) For corrected temperature, frequency-based indices and time series
308 performances are compared with observed temperature data. The frequency-based
309 indices include mean, median, standard deviation, and 10th, 90th percentiles while time
310 series based metrics include NS, P_{BIAS} , R^2 and MAE.

311 3) For simulated streamflow driven by corrected RCM simulations, the
312 frequency-based indices are visualized using boxplot, exceedance probability curve,
313 and exceedance probabilities of 7-day peak flow and low flow. Time series based
314 metrics include NS, P_{BIAS} , R^2 and MAE.

315

316 **4 Results**

317 4.1. Initial streamflow simulation driven with raw RCM simulations and sensitivity
318 analysis

319 To illustrate the necessity of bias correction in climate change impact on
320 hydrology, we re-calibrated SWAT using the raw RCM simulations while keeping all
321 SWAT parameters in their reasonable ranges. The assumption is that if the re-calibrated
322 hydrological model driven by the raw RCM simulations performs well and model
323 parameters are reasonable, then there is no need for bias correction. The streamflow
324 simulated by the re-calibrated model was plotted in Fig. 2, and it systematically
325 overestimates the observation a lot with NS equals to -6.65. Therefore, it is necessary
326 to correct the climate variables before they can be used for hydrological impact study.

327 And then the Sobol' method was applied to study which meteorological variables
328 should be corrected for hydrological modeling. Table 1 lists the sensitivity results for
329 these five meteorological variables. As it can be seen, precipitation is the most
330 sensitive (the main effect S_i is 44.0% and total effect S_{Ti} is 74.0%), followed by
331 temperature ($S_i = 15.0%$ and $S_{Ti} = 36.9%$) and solar radiation ($S_i = 7.7%$ and $S_{Ti} =$
332 22.6%), and the interactions between these factors are large. The relative humidity and
333 wind speed are insensitive in this case. This means precipitation, temperature and solar
334 radiation need to be bias corrected before applied to hydrologic models.

335

336 4.2 Evaluation of corrected precipitation and temperature

337 The bias correction was done on RCM simulated precipitation, minimum
338 temperature, maximum temperature, and solar radiation (for solar radiation, LS and
339 VARI methods were used) for two meteorological stations Bayanbulak and Baluntai.
340 Results show: 1) for solar radiation, there is no significant difference for different
341 correction methods. There the results are not shown. 2) Similar results were obtained
342 for minimum temperature and maximum temperature, and for Bayanbulak and
343 Baluntai. Therefore we only list and discuss results for Bayanbulak, and maximum
344 temperature.

345 Table 4 lists the frequency-based statistics of observed, raw RCM-simulated and
346 corrected precipitation data at the Bayanbulak Station. This station has a low
347 precipitation (daily mean 0.73mm or annual mean 266mm) and precipitation falls in 32%
348 days in a year with a mean intensity 2.3mm. Compared to the observation, the raw
349 RCM simulations deviate significantly from observation, with overestimation of all the
350 statistics. All the bias-correction methods improves the raw RCM simulated
351 precipitation, however, there are differences between their corrected statistics. LS
352 method has a good estimation of the mean while it shows a large bias in other
353 measures, e.g., it largely overestimated the probability of wet days (e.g., up to 41%
354 overestimation) and underestimated the standard deviation (up to 0.91 mm
355 underestimation). LOCI method provides a good estimation in the mean, median,
356 wet-day probability and wet-day intensity; however, there is a slight underestimation in
357 the standard deviation and therefore 90th percentile. Compared to LS and LOCI, PT

358 method performs well in all these metrics. In spite of slight better estimation of
359 standard deviation, probability of wet days and intensity of wet day, DM method has
360 an overestimation of the mean and an underestimation of standard deviation. This
361 means that precipitation does not follow the assumed Gamma distribution. On the
362 contrary, QM method doesn't have this assumption and it provides an excellent
363 estimation of these statistics. These results are consistent with previous studies
364 (Thieme et al., 2011; Thieme et al., 2012; Wilcke et al., 2013; Graham et al., 2007),
365 but are different from the research by Piani et al (2010) who found that performance of
366 DM method is unexpectedly well for the humid Europe region. This non-uniformity
367 can be partly attributed to the precipitation regime for different regions: better fit of the
368 assumed distribution lead to better performance of DM.

369

370 Table 5 lists the frequency-based statistics of observed, raw RCM simulated and
371 bias-corrected maximum temperature data at the Bayanbulak Station. The mean and
372 standard deviation are 3.08 and 14.5 °C, with the 90th percentile being 19.2 °C.
373 Analysis of the raw RCM simulations indicates deviation from observation, with an
374 overestimation of the mean, and underestimations of the median, standard deviation,
375 and 90th percentile. All three bias-correction methods corrected biases in RCM
376 simulated temperature and improved estimations of the statistics. LS has a correct
377 estimation of mean but a slight underestimation of median and standard deviation,
378 while VARI and DM have a good match with observations for all the frequency-based
379 statistics. These results are in accordance with Teutschbein and Seibert (2012), i.e., LS

380 method doesn't adjust the standard deviation and the 10th/90th percentiles while VARI
381 and DM methods do.

382

383 Figure 3 shows the exceedance probability curves of the observed and corrected
384 precipitation and temperature. For precipitation, the raw RCM simulations are heavily
385 biased (as also shown by statistics in Table 4). All correction methods effectively, but
386 in different extent, correct biases in raw precipitation. The LS method underestimates
387 the high precipitation with probability below 0.06 and overestimates the low
388 precipitation with probability between 0.06 ~ 0.32. The overestimation of precipitation
389 with probability between 0.32 ~ 0.73 indicates LS method has a very limited ability in
390 reproducing dry day precipitation (below 1 mm). Similar to LS method, the LOCI
391 method also overestimates the low precipitation with probability between 0.08 ~ 0.32
392 and underestimates the high precipitation with probability below 0.08. However, unlike
393 LS method, LOCI method performs well on the estimation of the dry days with
394 precipitation below 1 mm. The PT, DM and QM methods well adjust precipitation
395 exceedance except that DM method slightly overestimates the precipitation with
396 probability between 0.12 ~ 0.28. For temperature, the raw temperature overestimates
397 low temperature with probability above 0.65 and underestimates high temperature with
398 probability below 0.65. All temperature correction methods adjust the biases in raw
399 temperature and the corrected temperature has the similar quantiles with the
400 observation. They performed equally well and differences among each correction
401 method are negligible.

402

403 Time series based performances were evaluated and results are listed in Fig. 4 and
404 Table 6. For precipitation, all bias correction methods significantly improve the raw
405 RCM simulations. However, as shown in the right plot of Fig. 4, there is a systematic
406 mismatch between observation and corrections which follow the pattern of RCM
407 simulated precipitation. In addition, this mismatch differs between different methods,
408 among which the difference is smaller for LS and LOCI methods than for PT, DM, and
409 QM methods. This resulted in a slightly better squared difference based measures (e.g.,
410 NS, R^2) for LS and LOCI than PT, DM and QM methods, as indicated in Table 6.
411 Similar to precipitation, all correction methods significantly improved the raw RCM
412 simulated temperature. Differences between observation and raw temperature (e.g.,
413 1.1 °C in spring, 1.0 °C in summer, 3.3 °C in autumn, and up to 7.6 °C in winter) were
414 significantly corrected. These three correction methods performed equally well and no
415 significant differences exist between the average annual daily temperature graphs.

416

417 Table 6 lists performances of correction methods for monthly time series of
418 precipitation and temperature at the Bayanbulak Station. For precipitation, the
419 performance of the RCM simulated precipitation is very poor with NS=-6.78,
420 P_{BIAS} =293.28% and MAE=64.40 for monthly data, and the improvements of correction
421 are obvious. The " P_{BIAS} "s of the corrected precipitation are within $\pm 5\%$ and "NS"s
422 approach 0.64. It is worth noting that LS and LOCI methods perform better than PT
423 and QM methods in terms of time series performances. For temperature, although the

424 raw RCM simulation obtains an acceptable NS value (0.84), it severely overestimates
425 the observation ($P_{\text{BIAS}} = 15.78\%$ and $\text{MAE} = 4.31\text{ }^{\circ}\text{C}$). The “ P_{BIAS} ”s of the corrected
426 temperatures are within $\pm 5\%$ and “NS”s are over 94% (better than that of the “raw”)
427 for all three correction methods and there is no significant difference between these
428 results, which indicates the corrected monthly temperature series are in good
429 agreement with the observation.

430

431 4.3 Evaluation of streamflow simulations

432 Figure 5 compares the mean, median, first and third quantiles of daily observed
433 streamflows (“obs”) with simulated streamflows driven by observed meteorological
434 inputs (“default”), raw RCM simulations (“raw”), and 15 combinations of corrected
435 precipitation and corrected temperature (i.e., simulations 1 to 15). The overestimation
436 of simulated streamflow using raw RCM simulations (i.e., “raw”) is obvious. For
437 simulations 1 to 3, streamflow overestimations are also observed and they substantially
438 overestimate the mean streamflow by over 100%, while simulations 4 to 15 reproduce
439 similar streamflows as the observation or simulation “default”. As the major difference
440 between simulations 1 to 3 and other simulations is that simulations 1 to 3 use the
441 LS-corrected precipitation, this means precipitation corrected with LS method is not
442 suitable for flow simulation in this study.

443 To investigate the performances of bias correction methods for different
444 hydrological regimes, we divided the streamflow into two different periods according

445 to the hydrograph (Fig. 2): wet period is from April to September and dry period is
446 from October to March of next year. It is indicated that the performances of bias
447 correction methods are, except for magnitudes, similar for both wet and dry period (not
448 shown), which demonstrates that the evaluation is robust and can proved useful
449 information for both dry and wet season.

450 Figure 6 shows the exceedance probability curves (flow duration curves) of the
451 observed flow, and flows with simulation “default” and simulations 4 to 15. Generally
452 all simulations are in good agreement with the observation for frequencies between
453 0.12 and 0.72, and precipitation correction methods have more significant influence
454 than temperature correction methods. This confirms the previous sensitivity result that
455 precipitation is the most sensitive driving force to streamflow simulation. Similar to
456 performances of bias corrected precipitation, simulations with DM-corrected
457 precipitation (i.e. simulations 10 to 12) deviates the observation the most, followed
458 these with LOCI corrected precipitation (i.e., simulations 4 to 6), and then with PT
459 method and QM method. All simulations encounter the problem to correctly mimic the
460 low flow part (i.e. exceedance larger than 0.7). This might be a systematic problem of
461 the calibrated hydrologic model (as indicated by simulation “default”), e.g., the
462 objective function of the hydrological modeling is not focused on baseflow.
463 Differences among streamflows driven by different temperature but same precipitation
464 are insignificant. This result differs from the study of Teutschbien and Seibert (2012).
465 This may be related to the chosen RCM model or watershed characteristic.

466 The time series performances of simulation “default”, simulation “raw” and

467 simulations 1 to 15 at daily and monthly time steps are summarized in Table 3. The
468 “default” performs well with NS reaching 0.80 for daily and 0.90 for monthly
469 streamflow and daily MAE within 25 m³/s. The “raw” is heavily biased with NS close
470 to -53.4 and P_{BIAS} as large as 421 % for monthly data. All the 15 simulations improve
471 the statistics of the “raw” scenario significantly. For simulations 1 to 3, whose
472 precipitation series are corrected by LS method, NS ranges from -3.10 to -2.87 for
473 monthly streamflow and they substantially overestimate the streamflow with P_{BIAS}
474 over 110%. For simulations 4 to 15, monthly “NS”s are over 0.60, which indicates they
475 can reproduce satisfactory monthly streamflow in this watershed, and simulations with
476 precipitation corrected by LOCI (simulations 4 to 6) have best “NS”s and “P_{BIAS}”s.
477 However, these indices of daily streamflow are lower (the highest NS is 0.50 for
478 simulations 5 and 6), and this is related to the mismatch between corrected and
479 observed precipitation time series (see top plot in Figure 4), which is intrinsic from the
480 RCM model and cannot be improved through these correction methods.

481 It is worth noting that simulations 1 to 3 and simulations 4 to 6, whose
482 precipitation is corrected by LS and LOCI, respectively, vary significantly. The
483 difference between LS and LOCI is that LOCI introduces a threshold for the wet day
484 precipitation to correct the wet day probability while LS doesn't. That is a simple but
485 quite pragmatic approach since the raw RCM simulated precipitation usually has too
486 many drizzle days (Teutschbein and Seibert, 2012). Obviously, wet day probability is
487 crucial to streamflow simulation in this study.

488 Figure 7 shows the simulated monthly mean flow and exceedance probability

489 curves of 7-day peak and 7-day low flow. For the monthly mean streamflow, obviously
490 the “raw” is heavily biased with deviations ranging from 282% to 426%. Simulations 1,
491 2 and 3 also overestimate the observation, while simulations 4 to 15 reproduced good
492 monthly mean streamflow especially for simulations 4, 5 and 6. The annual peak flow
493 and low flow is presented in Fig. 7 to investigate the impact of bias correction methods
494 on extreme flows. For the peak flow, the exceedance probabilities of the simulations 4
495 to 15 are close to the observation while “raw” and simulations 1 to 3 deviate
496 significantly (not shown). It is worth noting that simulations 4, 5 and 6, which perform
497 the best in terms of the “NS”s, slightly underestimate the peak flow by 1% ~ 28%. The
498 reason may be that the LOCI method adjusts all precipitation events in a certain month
499 with a same scaling factor, which leads to the underestimation of the standard
500 deviation (Table 4) and high precipitation intensity, and finally results in an
501 underestimation of the peak streamflow. Results show slightly better performance of
502 PT, DM and QM methods than LOCI in predicting extreme flood, which is consistent
503 with previous study, e.g., Chen et al. (2013a) and Teutschbein and Seibert (2012), who
504 validated the effectiveness of bias correction methods for un-stationary conditions.

505 For the low flow, all simulations overestimate the observation, but are in good
506 agreement with the “default”, which can be attributed to the systematic deficit of the
507 hydrological model.

508 For the peak flow and low flow, both DM and QM methods perform well and QM
509 method is slightly better than DM method as the latter overestimates both peak flow
510 and low flow. However, there is an essential problem of QM method when comes to

511 correcting future climate since it fails to resolve the “new extreme” (modeled values
512 beyond the observed range) problem (Thiemeß et al., 2012) as the corrected
513 precipitation always falls between the maximum and minimum values.

514

515 **5 Conclusions**

516 This work compared the abilities of five precipitation bias correction methods and
517 three temperature bias correction methods in correcting RCM simulations for an arid
518 region. The evaluation includes their abilities to reproduce precipitation, temperature
519 and streamflow simulated using a hydrological model driven by corrected variables.

520 Sensitivity analysis shows precipitation is the most sensitive driving force to
521 streamflow simulation, followed by temperature and solar radiation, while relative
522 humidity and wind speed are not sensitive.

523 The raw RCM simulations are heavily biased from observed data, and this results
524 in biases in the simulated streamflows which cannot be corrected by model calibration;
525 and all bias correction methods effectively improve these simulations.

526 For precipitation, the PT and QM methods performed equally best in terms of the
527 frequency-based indices, (e.g., mean, standard deviation, percentiles); while LOCI
528 method performed best in terms of the time series based indices (e.g., NS, P_{BIAS} and
529 R^2).

530 For temperature, the raw RCM simulated temperature is highly relevant to the
531 observation but generally biased ($R^2 = 0.88$ and $P_{BIAS} = 15.78\%$ for monthly data). All

532 correction methods effectively corrected biases in the raw RCM simulated temperature
533 and they performed almost equally well for both frequency-based indices and time
534 series based indices.

535 For simulated streamflow, precipitation correction methods have more significant
536 influence than temperature correction methods and their performances of streamflow
537 simulations are consistent with these of corrected precipitation, i.e., PT and QM
538 methods performed equally best in correcting flow duration curve and peak flow while
539 LOCI method performed best in terms of the time series based indices (e.g., $NS = 0.69$,
540 $|P_{BIAS}| < 5\%$). Besides, the wet day probability is vital in simulating streamflow in this
541 study and it is recommended the LOCI method be applied to correct precipitation prior
542 to the correction by PT method.

543 This study also stresses the need for bias correction when assessing the impact of
544 climate change on hydrology using the RCM simulations. The most appropriate bias
545 correction method for RCM simulations may differ regarding to climate conditions or
546 evaluation indices. As such, it is necessary to find an appropriate bias correction
547 method based on the study purpose.

548 **Acknowledgment**

549 The research was supported by the “Thousand Youth Talents” Plan (Xinjiang Project)
550 and the National Basic Research Program of China (973 Program: 2010CB951003).
551 We wish to thank Prof. Gao X at National Climate Center (China) for providing the
552 output of Regional Climate Model used in this paper.

553

554 **References**

- 555 Ahmed, K. F., Wang, G., Silander, J., Wilson, A. M., Allen, J. M., Horton, R., and Anyah, R.: Statistical downscaling
556 and bias correction of climate model outputs for climate change impact assessment in the US northeast, *Global*
557 *Planet Change*, 100, 320-332, 2013.
- 558 Anderson, W. P., Jr., Storniolo, R. E., and Rice, J. S.: Bank thermal storage as a sink of temperature
559 surges in urbanized streams, *J Hydrol*, 409, 525-537, 10.1016/j.jhydrol.2011.08.059, 2011.
- 560 Arnell, N. W.: Factors controlling the effects of climate change on river flow regimes in a humid
561 temperate environment, *J Hydrol*, 132, 321-342, [http://dx.doi.org/10.1016/0022-1694\(92\)90184-W](http://dx.doi.org/10.1016/0022-1694(92)90184-W),
562 1992
- 563 Arnold, J., Muttiyah, R., Srinivasan, R., and Allen, P.: Regional estimation of base flow and groundwater
564 recharge in the Upper Mississippi river basin, *J Hydrol*, 227, 21-40, 2000.
- 565 Arnold, J. G., Srinivasan, R., Muttiyah, R. S., and Williams, J.: Large area hydrologic modeling and
566 assessment part I: Model development1, *JAWRA Journal of the American Water Resources*
567 *Association*, 34, 73-89, 1998.
- 568 Arnold, J. G., and Fohrer, N.: SWAT2000: current capabilities and research opportunities in applied
569 watershed modelling, *Hydrol Process*, 19, 563-572, 10.1002/hyp.5611, 2005.
- 570 Bergstrom, S., Carlsson, B., Gardelin, M., Lindstrom, G., Pettersson, A., and Rummukainen, M.:
571 Climate change impacts on runoff in Sweden-assessments by global climate models, dynamical
572 downscaling and hydrological modelling, *Climate Res*, 16, 101-112, 2001.
- 573 Block, P. J., Souza Filho, F. A., Sun, L., and Kwon, H. H.: A Streamflow Forecasting Framework using
574 Multiple Climate and Hydrological Models1, *JAWRA Journal of the American Water Resources*
575 *Association*, 45, 828-843, 2009.
- 576 Buytaert, W., Vuille, M., Dewulf, A., Urrutia, R., Karmalkar, A., and Celleri, R.: Uncertainties in climate
577 change projections and regional downscaling in the tropical Andes: implications for water resources
578 management, *Hydrol Earth Syst Sc*, 14, 1247-1258, 10.5194/hess-14-1247-2010, 2010.
- 579 Chen, J., Brissette, F. P., Chaumont, D., and Braun, M.: Finding appropriate bias correction methods in
580 downscaling precipitation for hydrologic impact studies over North America, *Water Resour Res*, 49,
581 4187-4205, 10.1002/wrcr.20331, 2013a.
- 582 Chen, Y., Xu, C., Chen, Y., Li, W., and Liu, J.: Response of glacial-lake outburst floods to climate
583 change in the Yarkant River basin on northern slope of Karakoram Mountains, China, *Quaternary*
584 *International*, 226, 75-81, 2010.
- 585 Chen, Y., Du, Q., and Chen, Y.: Sustainable water use in the Bosten Lake Basin, Science press, Beijing,
586 329 pp., 2013b.
- 587 Chen, Z., Chen, Y., and Li, B.: Quantifying the effects of climate variability and human activities on
588 runoff for Kaidu River Basin in arid region of northwest China, *Theoretical and applied*
589 *climatology*, 111, 537-545, 2013c.
- 590 Elguindi, N., Somot, S., Déqué M., and Ludwig, W.: Climate change evolution of the hydrological
591 balance of the Mediterranean, Black and Caspian Seas: impact of climate model resolution, *Clim*
592 *Dynam*, 36, 205-228, 2011.
- 593 Fang, G., Yang, J., Chen, Y., Xu, C.: Contribution of meteorological input in calibrating a distributed
594 hydrologic model with the application to a watershed in the Tianshan Mountains, China, *Environ*
595 *Earth Sci*, submitted Sep, 2014, under submission.

596 Fowler, H. J., Ekström, M., Blenkinsop, S., and Smith, A. P.: Estimating change in extreme European
597 precipitation using a multimodel ensemble, *J Geophys Res*, 112, D18, 2007.

598 Gao, X., Wang, M., and Giorgi, F.: Climate change over China in the 21st century as simulated by
599 BCC_CSM1.1-RegCM4.0, *Atmos. Oceanic Sci. Lett*, 6, 381-386, 2013.

600 Giorgi, F.: Simulation of regional climate using a limited area model nested in a general circulation
601 model, *Journal of Climate* 3, 941-963, 1990.

602 Giorgi, F., and Mearns, L. O.: Introduction to special section: Regional climate modeling revisited,
603 *Journal of Geophysical Research: Atmospheres* (1984–2012), 104, 6335-6352, 1999.

604 Graham, L. P., Andréasson, J., and Carlsson, B.: Assessing climate change impacts on hydrology from
605 an ensemble of regional climate models, model scales and linking methods—a case study on the
606 Lule River basin, *Climatic Change*, 81, 293-307, 2007.

607 Lenderink, G., Buishand, A., and Deursen, W. v.: Estimates of future discharges of the river Rhine using
608 two scenario methodologies: direct versus delta approach, *Hydrol Earth Syst Sc*, 11, 1145-1159,
609 2007.

610 Li, B., Chen, Y., and Shi, X.: Why does the temperature rise faster in the arid region of northwest China?,
611 *J Geophys Res*, 117, 2012.

612 Liu, T., Willems, P., Pan, X. L., Bao, A. M., Chen, X., Veroustraete, F., and Dong, Q. H.: Climate change
613 impact on water resource extremes in a headwater region of the Tarim basin in China, *Hydrol Earth
614 Syst Sc*, 15, 3511-3527, 10.5194/hess-15-3511-2011, 2011.

615 Liu, Z., Xu, Z., Huang, J., Charles, S. P., and Fu, G.: Impacts of climate change on hydrological
616 processes in the headwater catchment of the Tarim River basin, China, *Hydrol Process*, 24, 196-208,
617 10.1002/hyp.7493, 2010.

618 Maraun, D., Wetterhall, F., Ireson, A. M., Chandler, R. E., Kendon, E. J., Widmann, M., Brienen, S.,
619 Rust, H. W., Sauter, T., Themeßl, M., Venema, V. K. C., Chun, K. P., Goodess, C. M., Jones, R. G.,
620 Onof, C., Vrac, M., and Thiele-Eich, I.: Precipitation downscaling under climate change: recent
621 developments to bridge the gap between dynamical models and the end user, *Rev Geophys*, 48,
622 RG3003, 2010.

623 Mehrotra, R., and Sharma, A.: An improved standardization procedure to remove systematic low frequency
624 variability biases in GCM simulations, *Water Resour Res*, 48, W12601, 10.1029/2012WR012446, 2012.

625 Murphy, J.: An evaluation of statistical and dynamical techniques for downscaling local climate, *Journal
626 of Climate*, 12, 2256-2284, 1999.

627 Nash, J. E., and Sutcliffe, J.: River flow forecasting through conceptual models part I—A discussion of
628 principles, *J Hydrol*, 10, 282-290, 1970.

629 Piani, C., Haerter, J., and Coppola, E.: Statistical bias correction for daily precipitation in regional
630 climate models over Europe, *Theoretical and Applied Climatology*, 99, 187-192, 2010.

631 Schmidli, J., Frei, C., and Vidale, P. L.: Downscaling from GC precipitation: A benchmark for dynamical
632 and statistical downscaling methods, *International Journal of Climatology*, 26, 679-689,
633 10.1002/joc.1287, 2006.

634 Seager, R., and Vecchi, G. A.: Greenhouse warming and the 21st century hydroclimate of southwestern
635 North America, *Proc. Natl. Acad. Sci. U. S. A.*, 107, 21277-21282, 10.1073/pnas.0910856107,
636 2010.

637 Setegn, S. G., Rayner, D., Melesse, A. M., Dargahi, B., and Srinivasan, R.: Impact of climate change on
638 the hydroclimatology of Lake Tana Basin, Ethiopia, *Water Resour Res*, 47, W04511,
639 10.1029/2010WR009248, 2011.

640 Shen, Y., and Chen, Y.: Global perspective on hydrology, water balance, and water resources
641 management in arid basins, *Hydrol Process*, 24, 129-135, 2010.

642 Sobol', I. M.: Global sensitivity indices for nonlinear mathematical models and their Monte Carlo
643 estimates, *Math Comput Simulat*, 55, 271-280, 10.1016/s0378-4754(00)00270-6, 2001.

644 Sun, F., Roderick, M. L., Lim, W. H., and Farquhar, G. D.: Hydroclimatic projections for the
645 Murray-Darling Basin based on an ensemble derived from Intergovernmental Panel on Climate
646 Change AR4 climate models, *Water Resour Res*, 47, W00G02, 10.1029/2010wr009829, 2011.

647 Sun, G., Chen, Y., Li, W., Pan, C., Li, J., and Yang, Y.: Spatial distribution of the extreme hydrological
648 events in Xinjiang, north-west of China, *Nat Hazards*, 67, 483-495, 2013.

649 Terink, W., Hurkmans, R., Torfs, P., and Uijlenhoet, R.: Evaluation of a bias correction method applied
650 to downscaled precipitation and temperature reanalysis data for the Rhine basin, *Hydrology &
651 Earth System Sciences*, 14, 687-703, 2010.

652 Teutschbein, C., and Seibert, J.: Bias correction of regional climate model simulations for hydrological
653 climate-change impact studies: Review and evaluation of different methods, *J Hydrol*, 456, 12-29,
654 10.1016/j.jhydrol.2012.05.052, 2012.

655 Themeßl, M. J., Gobiet, A., and Leuprecht, A.: Empirical - statistical downscaling and error correction
656 of daily precipitation from regional climate models, *International Journal of Climatology*, 31,
657 1530-1544, 2011.

658 Themeßl, M. J., Gobiet, A., and Heinrich, G.: Empirical-statistical downscaling and error correction of
659 regional climate models and its impact on the climate change signal, *Climatic Change*, 112,
660 449-468, 2012.

661 Thom, H. C.: A note on the gamma distribution, *Mon Weather Rev*, 86, 117-122, 1958.

662 Wang, H., Chen, Y., Li, W., and Deng, H.: Runoff responses to climate change in arid region of
663 northwestern China during 1960–2010, *Chinese Geographical Science*, 23, 286-300, 2013.

664 Wilcke, R. A. I., Mendlik, T., and Gobiet, A.: Multi-variable error correction of regional climate models,
665 *Climatic Change*, 120, 871-887, 2013.

666 Wu, T., Li, W., Ji, J., Xin, X., Li, L., Wang, Z., Zhang, Y., Li, J., Zhang, F., and Wei, M.: Global carbon
667 budgets simulated by the Beijing Climate Center Climate System Model for the last century,
668 *Journal of Geophysical Research: Atmospheres*, 118, 4326-4347, 2013.

669 Xin, X., Wu, T., Li, J., Wang, Z., Li, W., and Wu, F.: How well does BCC_CSM1.1 reproduce the 20th
670 century climate change over China, *Atmos. Oceanic Sci. Lett*, 6, 21-26, 2013.

671 Xu, C., Chen, Y., Chen, Y., Zhao, R., and Ding, H.: Responses of Surface Runoff to Climate Change and
672 Human Activities in the Arid Region of Central Asia: A Case Study in the Tarim River Basin, China,
673 *Environ Manage*, 51, 926-938, 2013.

674

675

676 **Table 1.** Sensitivity indices of the five meteorological variables based on the Sobol' method.

Factor	Meaning	Factor range	Main effect S_i (%)	Total effect S_{Ti} (%)
a__tmp	Additive change to temperature	[-5,5]	15.0	36.9
r__pcp	Relative change to precipitation	[-0.5,0.5]	44.0	74.0
r__hmd	Relative change to humidity	[-0.5,0.5]	0.0	0.0
r__slr	Relative change to solar radiation	[-0.5,0.5]	7.7	22.6
r__wnd	Relative change to wind speed	[-0.5,0.5]	0.3	0.9

677

678

679

680

681

682 **Table 2.** Bias correction methods for RCM-simulated precipitation and temperature.

Bias correction for precipitation	Bias correction for temperature
Linear Scaling (LS)	Linear Scaling (LS)
LOCAl Intensity scaling (LOCI)	VARIance scaling (VARI)
Power Transformation (PT)	Distribution Mapping for temperature using Gaussian distribution (DM)
Distribution Mapping for precipitation using Gamma distribution (DM)	
Quantile Mapping (QM)	

683

684

685 **Table 3.** Performances of simulated streamflows driven by observed (default), raw RCM-simulated
686 (raw), and 15 combinations of bias-corrected precipitation and temperature during the period 1986
687 ~ 2001. For all combinations, solar radiation is corrected with Linear Scaling (LS) method. (Values
688 are given with one decimal except for NS).

Bias correction method			Daily				Monthly			
Precipitation	Temperature		NS	P _{BIAS}	R ²	MAE (m ³ /s)	NS	P _{BIAS}	R ²	MAE (m ³ /s)
default	obs	obs	0.80	4.3	0.8	24.2	0.90	4.3	0.9	16.6
raw	raw	raw	-44.91	420.5	0.4	487.9	-53.35	421.1	0.6	487.0
1	LS	LS	-2.65	115.6	0.5	136.4	-3.10	115.8	0.7	134.0
2	LS	VARI	-2.43	112.7	0.5	133.3	-2.87	113.0	0.7	130.6
3	LS	DM	-2.43	112.7	0.5	133.3	-2.87	113.0	0.7	130.6
4	LOCI	LS	0.49	-3.7	0.5	35.9	0.69	-3.7	0.7	25.3
5	LOCI	VARI	0.50	-4.5	0.5	35.6	0.69	-4.4	0.7	25.4
6	LOCI	DM	0.50	-4.5	0.5	35.6	0.69	-4.4	0.7	25.4
7	PT	LS	0.37	1.1	0.4	40.1	0.62	1.1	0.6	28.7
8	PT	VARI	0.38	0.3	0.4	39.8	0.63	0.3	0.6	28.6
9	PT	DM	0.38	8.3	0.5	41.2	0.62	8.3	0.7	30.6
10	DM	LS	0.40	7.5	0.5	40.7	0.63	6.7	0.6	30.3
11	DM	VARI	0.40	7.5	0.5	40.7	0.63	5.9	0.6	30.3
12	DM	DM	0.38	0.3	0.4	39.8	0.63	5.9	0.6	28.6
13	QM	LS	0.37	1.8	0.4	39.9	0.63	1.9	0.6	28.6
14	QM	VARI	0.38	1.0	0.4	39.5	0.63	1.0	0.6	28.4
15	QM	DM	0.38	1.0	0.4	39.5	0.63	1.0	0.6	28.4

689

690 **Table 4.** Frequency-based statistics of daily observed (“obs”), raw RCM-simulated (“raw”) and
 691 bias-corrected precipitations at the Bayanbulak Station (values are given with two decimal digits).

	Mean (mm)	Median (mm)	Standard deviation (mm)	90 th percentile (mm)	Probability of wet days (%)	Intensity of wet day (mm)
obs	0.73	0.00	2.44	1.90	32	2.30
raw	2.87	1.44	4.09	7.44	86	3.34
LS	0.73	0.20	1.53	2.10	73	1.00
LOCI	0.73	0.00	1.70	2.40	32	2.29
PT	0.73	0.00	2.44	1.80	32	2.30
DM	0.78	0.00	2.30	2.11	32	2.46
QM	0.73	0.00	2.44	1.90	32	2.31

692

693

694

695

696

697 **Table 5.** Frequency based statistics (unit: °C) of daily observed (“obs”), raw RCM simulated
 698 (“raw”) and bias corrected maximum temperatures at the Bayanbulak Station (values are given with
 699 two decimals).

	Mean	Median	Standard deviation	10 th percentile	90 th percentile
obs	3.08	7.20	14.50	-18.70	19.20
raw	3.45	3.21	10.88	-10.34	17.90
LS	3.08	6.65	14.14	-17.33	19.40
VARI	3.08	6.85	14.50	-17.76	19.36
DM	3.08	6.85	14.50	-17.76	19.36

700

701 **Table 6.** Time series based metrics of bias-corrected precipitation and temperature calculated on a
 702 monthly scale at the Bayanbulak Station (values are given with two decimals).

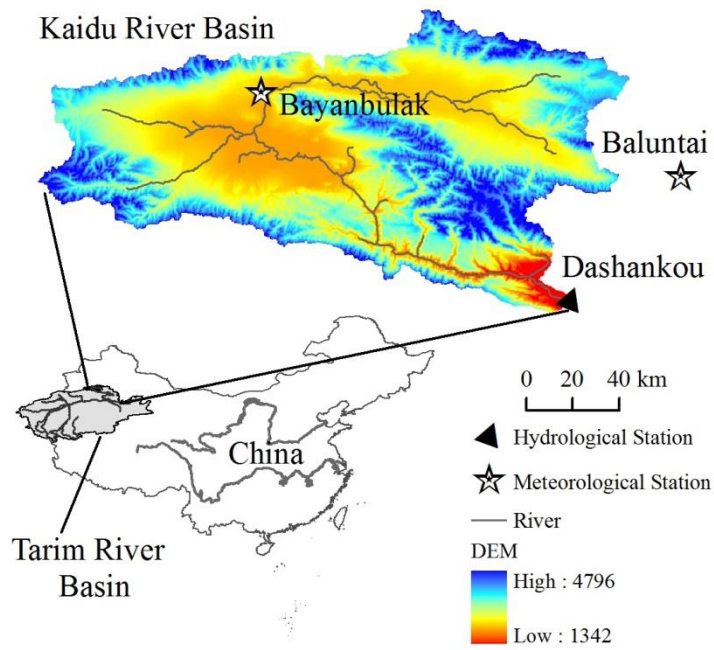
		NS	P _{BIAS} (%)	R ²	MAE (mm or °C)
Precipitation	raw	-6.78	293.28	0.42	65.40
	LS	0.64	0.06	0.65	9.66
	LOCI	0.61	-0.71	0.64	10.14
	PT	0.42	-0.09	0.53	11.98
	DM	0.46	6.64	0.56	11.78
	QM	0.44	0.03	0.54	11.99
Temperature	raw	0.84	15.78	0.88	4.31
	LS	0.95	3.04	0.95	2.35
	VARI	0.94	4.78	0.94	2.52
	DM	0.94	4.74	0.94	2.52

703

704

705

706

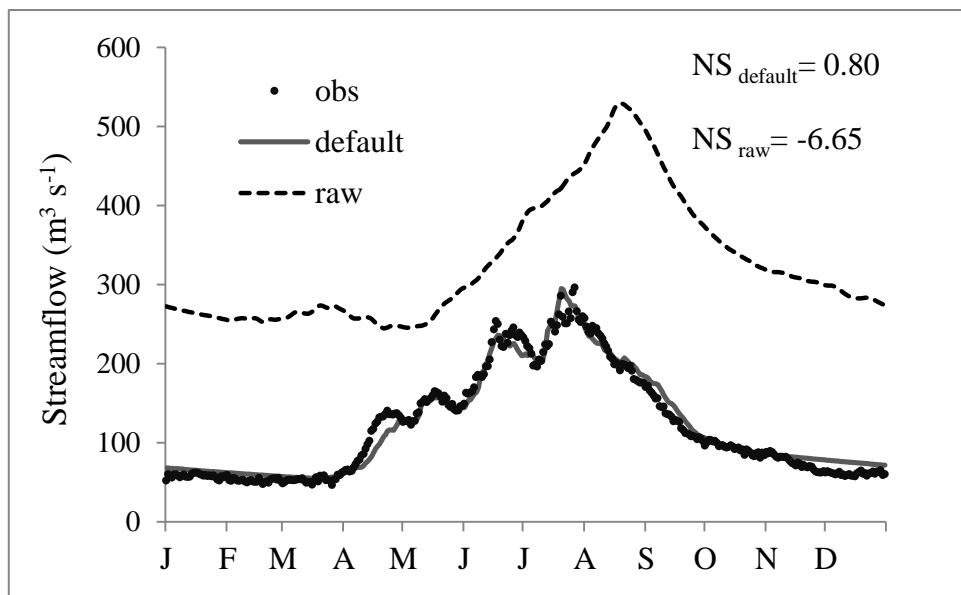


707

708 **Fig. 1.** Location of the study area, two meteorological stations and one hydrological station.

709

710

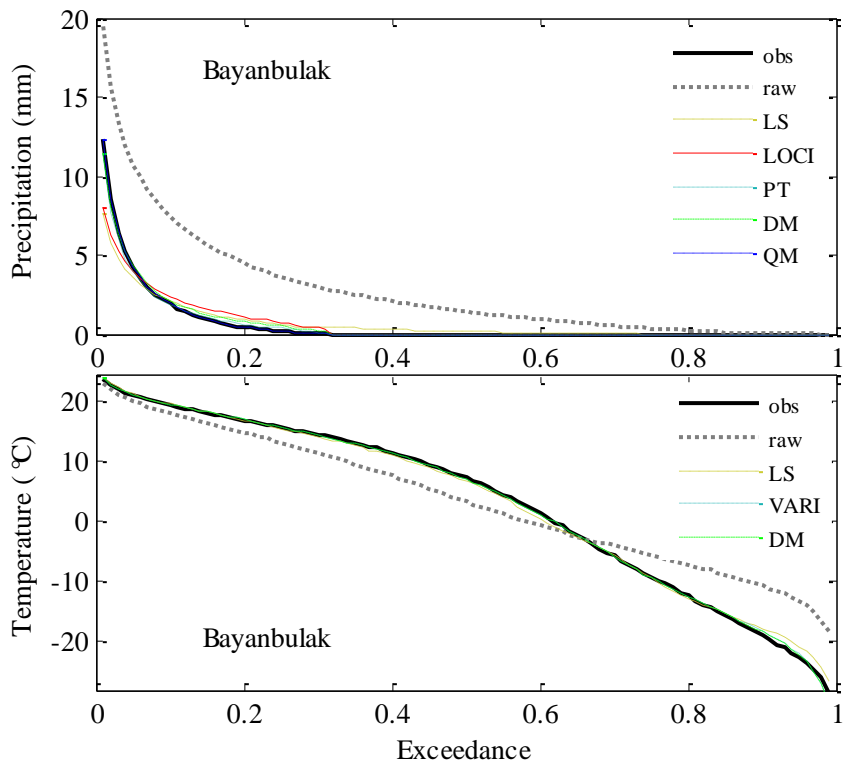


711

712 **Fig. 2.** Mean annual hydrographs of observed streamflow (“obs”) and simulated streamflow using
713 observed meteorological data (“default”) during the period of 1986 ~ 2001 at the Dashankou
714 Station. The simulated streamflow using raw RCM-simulated meteorological data after
715 re-calibration (“raw”) is also plotted. The NS values are for the daily continuous data and not for
716 the mean hydrograph.

717

718

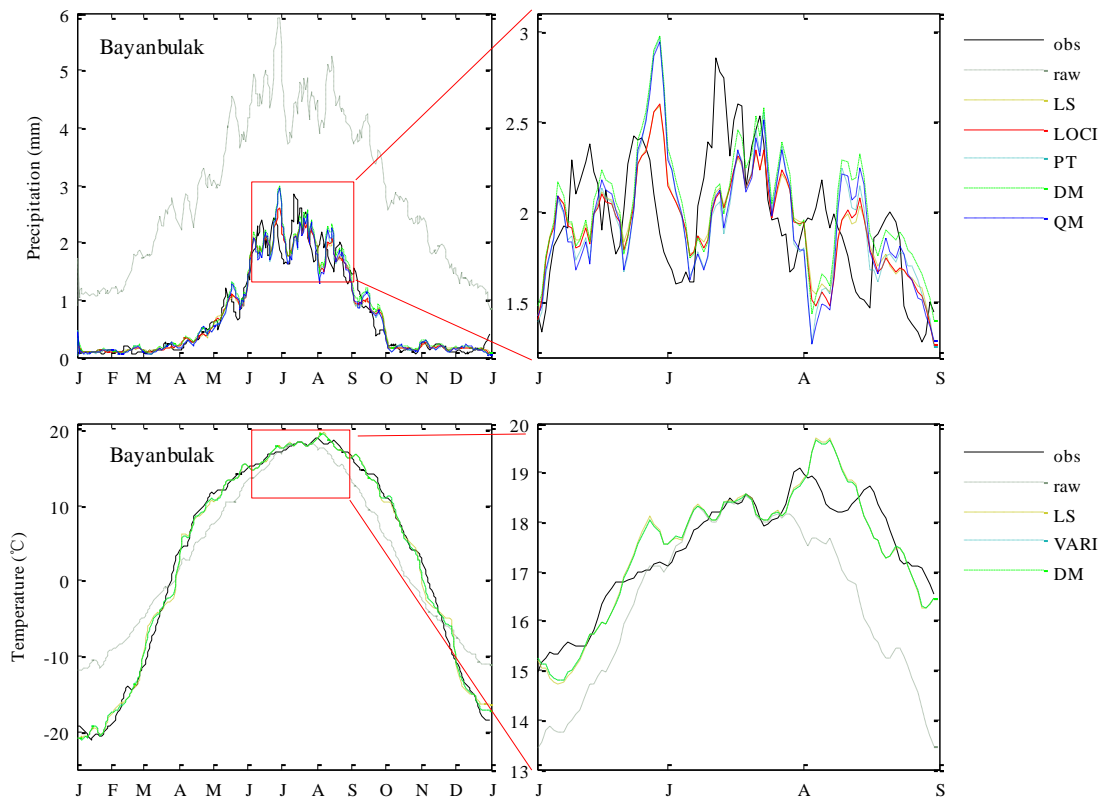


720

721 **Fig. 3.** Exceedance probabilities of the observed (“obs”), raw, and bias-corrected precipitation (top)
 722 and temperature (bottom) at the Bayanbulak Station.

723

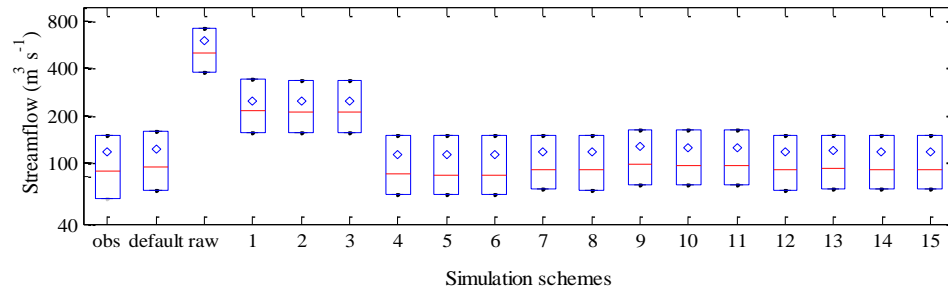
724



725

726 **Fig. 4.** Average precipitation and temperature hydrographs of observed (“obs”), raw RCM
 727 simulated (“raw”), and bias corrected values at Bayanbulak Station, which were smoothed with
 728 7-day moving average method. The precipitation and temperature during May to August is
 729 amplified to inspect the performance of each correction method.

730

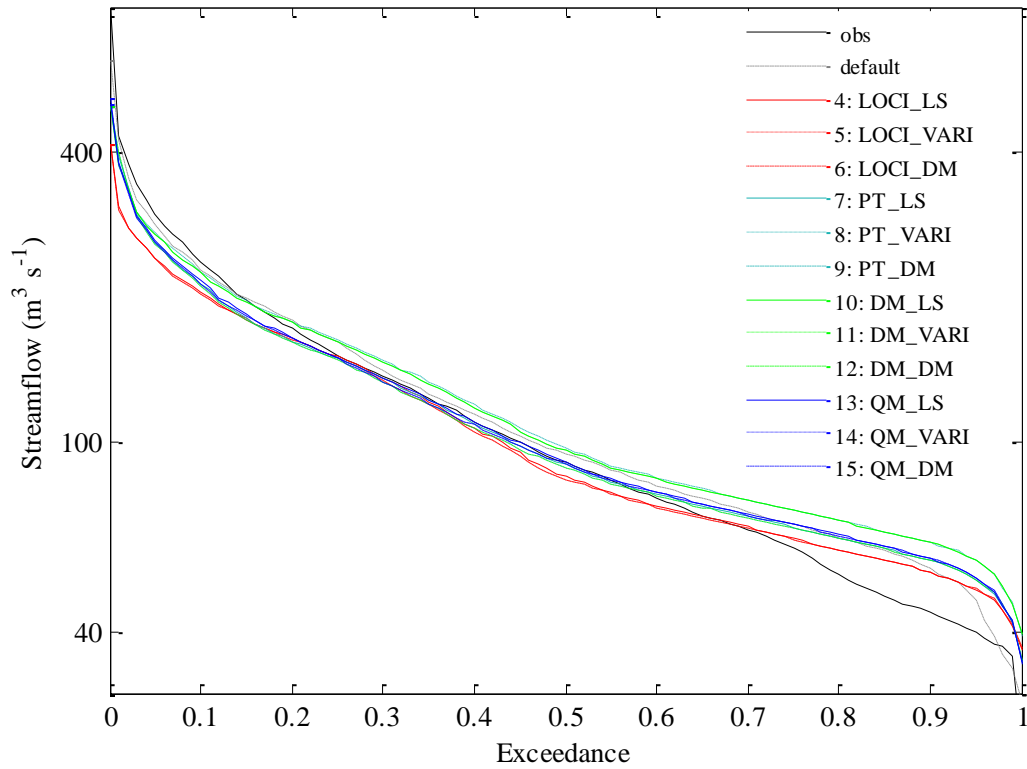


731

732 **Fig. 5.** Box plots of observed (“obs”) and simulated daily streamflows using observed (“default”),
 733 raw RCM simulated (“raw”) and corrected meteorological data (numbers from 1 to 15; see Table 3
 734 for setup of these 15 simulations). Solid boxes signify values from 1st to 3rd quantile while the
 735 median value is shown in the interior of the box, and the mean values are shown with diamonds.

736

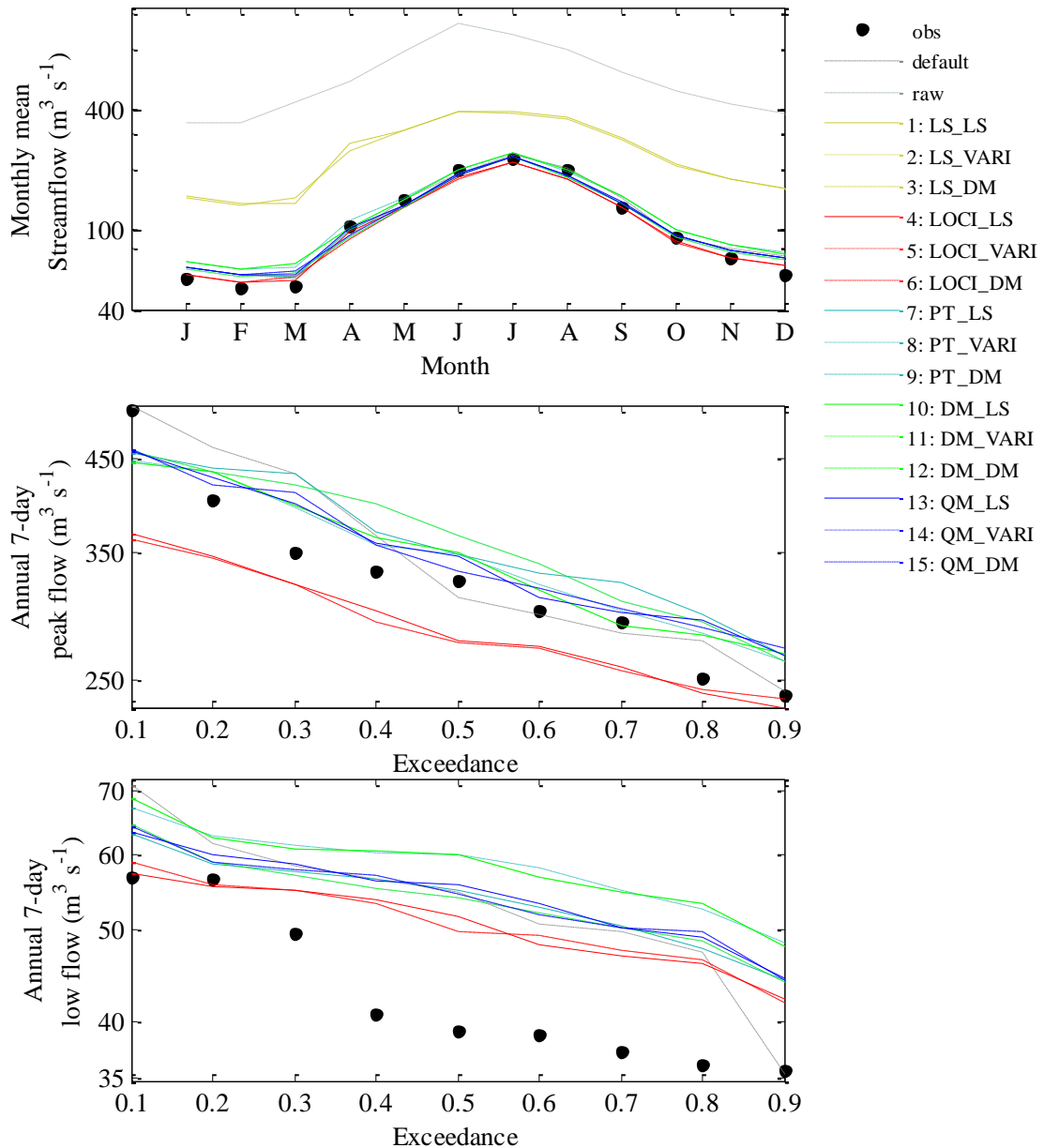
737



739

740 **Fig. 6.** Exceedance probability curves of observed (“obs”) and simulated streamflow driven by
 741 observed (“default”), and bias-corrected meteorological data (numbers from 4 to 15; also see Table
 742 3 for detail setup of these 12 simulations) For plotting purpose, simulations “raw” and 1 to 3 are not
 743 shown.

744



745
 746 **Fig. 7.** Monthly mean streamflow (top) and exceedance probability curves of annual 7-day peak
 747 flow (middle) and annual 7-day low flow (bottom) during 1986 ~ 2001 in the Kaidu River Basin.
 748 The observation (“obs”), and simulated streamflows using observed (“default”), raw
 749 RCM-simulated (“raw”) and bias-corrected (numbers from 1 to 15; also see Table 3 for detail setup
 750 of these 15 simulations) meteorological data are also shown in the monthly mean plot. For peak
 751 flow and low flow, the raw and simulations 1 to 3 are not shown as they are heavily biased.

752
 753